10A.6 S-BAND RADAR DUAL POLARIZATION OBSERVATIONS OF WINTER STORMS

P. C. Kennedy* and S. A. Rutledge
Colorado State University, Fort Collins, Colorado

1. INTRODUCTION

The CSU-CHILL radar has collected data from a number of winter storms that have affected northeastern Colorado in recent years. These have primarily been target of opportunity operations in which various dual polarization data collection procedures and antenna scanning patterns have been tested. Examinations of the resultant data archives reveal characteristic patterns in the dual polarization data fields observed during major winter storms. The pattern of interest in this paper is the development of mesoscale regions of modest S-Band specific propagation phase (Kdp) values (~0.2 - 0.6^o km^{-1}) that occur near the -15^{o}C environmental temperature level; a feature that has been noted by Trapp et al. (2001). The vertical stratification of additional radar data fields (primarily reflectivity and differential reflectivity (Zdr)) imply that the elevated maximum Kdp layer is associated with active ice crystal growth and aggregation processes. A radar backscattering model is used to gain additional insights into the dual polarization data values expected from various populations of crystaline and low density aggregate-type ice particles.

The radar data were collected by the 11 cm wavelength CSU-CHILL National Radar Facility located near Greeley, Colorado at an elevation of 1432 m MSL. At the time of these observations, the antenna was a center-fed 8.5m parabolic design with a 3dB beamwidth of ~1.0^o. (This antenna has since been replaced with an offset feed design; see paper P8.3 in this conference volume.) Identical Klystron-based FPS-18 transmitters are used to drive the antenna's horizontal (H) and vertical (V) ports. The data presented here were collected with the transmit polarization alternating between H and V on a pulse to pulse basis. Scan rates were typically 6 – 10^{o}sec^{-1} during PPI scans and ~1^{o}sec^{-1} during RHI scans. (For additional information on the radar please see web site: chill.colostate.edu).

Positive differential propagation phase shifts (increasing phase lag of the H return signal with respect to the V signal) arise from the collective effects of oblate scatterers along the radar beam path.

*Corresponding author address: Patrick C. Kennedy, Dept. of Atmospheric Science, Colorado State University, Fort Collins, CO 80523. email: pat@chill.colostate.edu

Various procedures have been developed for calculating Kdp; the range derivative of the phidp profile. In this paper, Kdp was calculated using the methods of Wang and Chandrasekar, 2009.

2. 20 DECEMBER 2006 STORM OBSERVATIONS

Around 1500 UTC of the morning of 20 December 2006 heavy snow and high surface wind conditions began to overspread much of the greater Denver area in northeastern Colorado. Between 1437 and 1504 UTC the METAR surface observations made at Denver International Airport (KDEN) first began to include heavy snow; prevailing visibilities decreased to 1/8 statute mile during this time period. By 22 UTC airport operations were completely suspended due to the continuing heavy accumulating and drifting snow.

Figure 1a shows the reflectivity pattern observed in a 3.5^o elevation angle PPI scan at 1419 UTC. To aid contour plotting, the data have been interpolated to a 1 km by 1 km X, Y grid on the PPI scan surface using the NCAR sorted position radar interpolation program (SPRINT; Mohr and Vaughan 1979; Miller et al., 1986). The grid origin is at the CSU-CHILL radar (marked as CHL); KDEN is located near X=-3, Y=-65 km. The three range rings have been added to indicate the distances at which the beam height reached the -10, -15, and -20^{o}c temperature levels according to the 12 UTC Denver radiosonde data. At 1419 UTC, the strongest reflectivities were generally located east of the CHL - KDEN line.

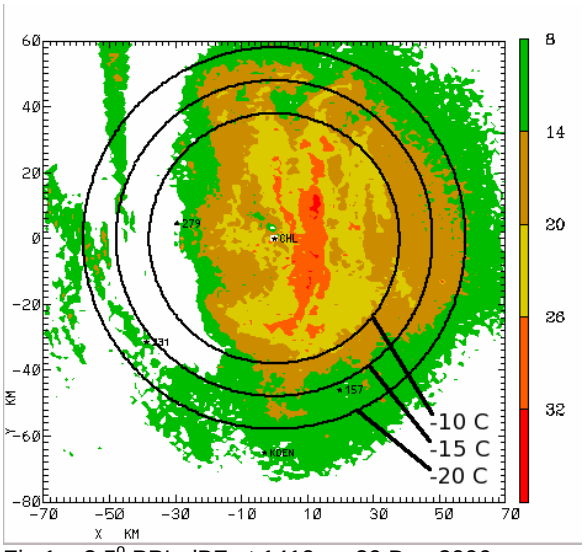

Fig 1a: 3.5^o PPI: dBZ at 1419 on 20 Dec 2006

Figure 1b shows the 3.5° elevation angle Kdp field at 1419. (The Kdp values have been scaled up by a factor of 10; a color scale value of 2 indicates a Kdp of 0.2 °km^{-1}). At this time, the largest region of Kdp values of 0.2°km^{-1} or more was located in a small area centered near X=40, Y=-20 km; the temperature rings indicate that this positive Kdp region was near the -15° C temperature level.

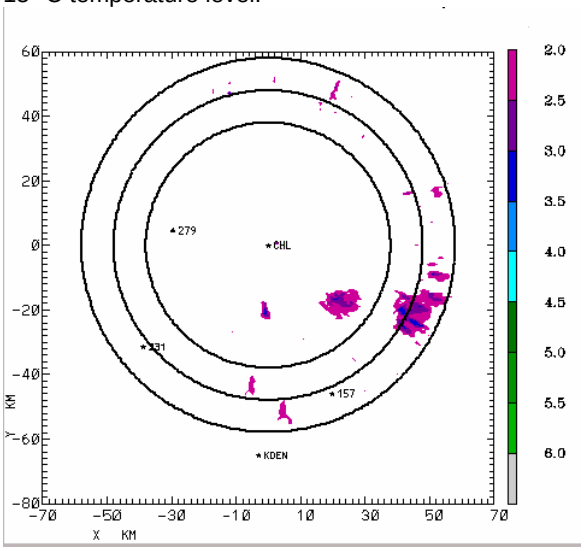

Fig 1b: As in Fig1a except data is Kdp x 10.

The evolution of the reflectivity and Kdp patterns on the 3.5° PPI surface over the next 45 minutes is shown in Fig. 2a. At 1505, reflectivities exceeding 20 dBZ had expanded appreciably to the west of the CHL – KDEN line. The associated Kdp plot showed that the region containing >0.2°km^{-1} values had increased considerably in the CHILL's southeast azimuth quadrant (Fig. 2b). Within this expanding area, the maximum Kdp values remained in fairly close proximity to the -15°C altitude.

The radial velocity pattern at 1504 (Fig. 3) provides a sense of the trajectories of the hydrometeors that were causing the increasingly heavy snow reported at KDEN at this time. Approximately 20 ms-1 northerly flow near the surface veered towards the northeast at the height of the -15°C level (~3 km AGL). In this strong horizontal wind field, snow particles located at a height of 3 km would have ~60 km long trajectories as they fell to the surface (assuming a fall speed of 1 ms^{-1}). The diverging line segments added to Fig. 3 indicate the expected source direction for the snow particles reaching KDEN. These inferred trajectories suggest that the heavy snow at KDEN may have been connected to the expanding "upstream" positive Kdp area near the -15°C level.

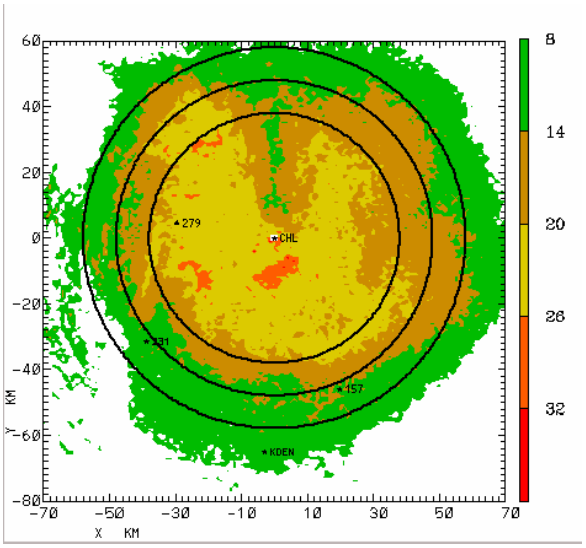

Fig 2a: 3.5° PPI: dBZ at 1504 on 20 Dec 2006

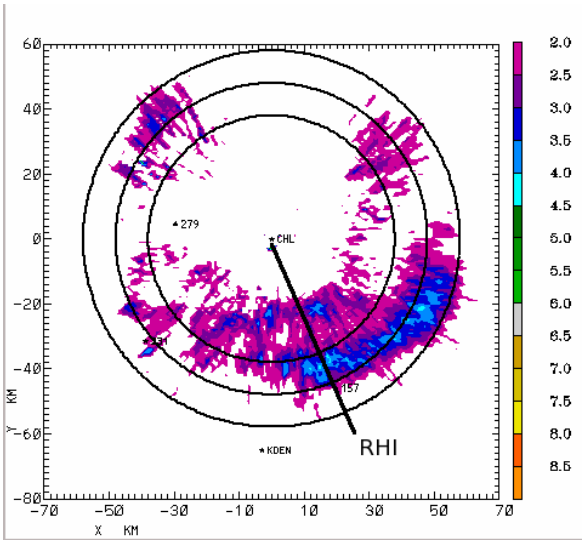

Fig. 2b: As in 2a except data is Kdp x 10

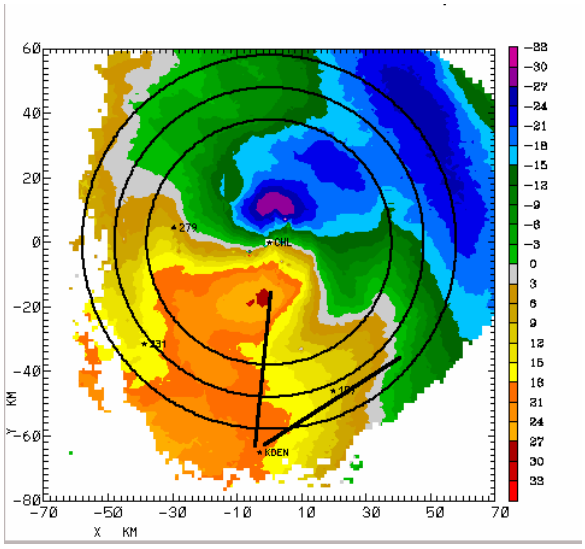

Fig 3: As in 2a except data is unfolded radial velocity in ms^{-1}.

RHI scans along the ~157 degree azimuth provide a more detailed view of the Kdp pattern evolution in the vertical. At 1424 extensive snow echo was present in this RHI plane (Fig. 4a) The increasing reflectivity with decreasing height is a typical signature of snow particle aggregation (Ryzhkov and Zrnic, 1988). The associated Kdp field contains patchy indications of a $>0.2^{o}km^{-1}$ layer located just below 3 km AGL (Fig. 4b). At 1502 The depth of the surface-based >15 dBZ echo layer had increased (Fig. 5a). The enhanced elevated Kdp layer expanded and intensified between 1442 and 1502 UTC (Fig. 5b).

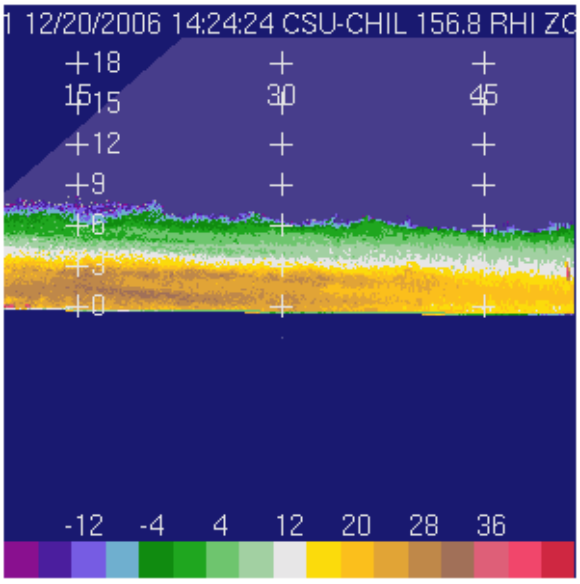

Fig 4a: dBZ RHI 1424 UTC 20 Dec 2006

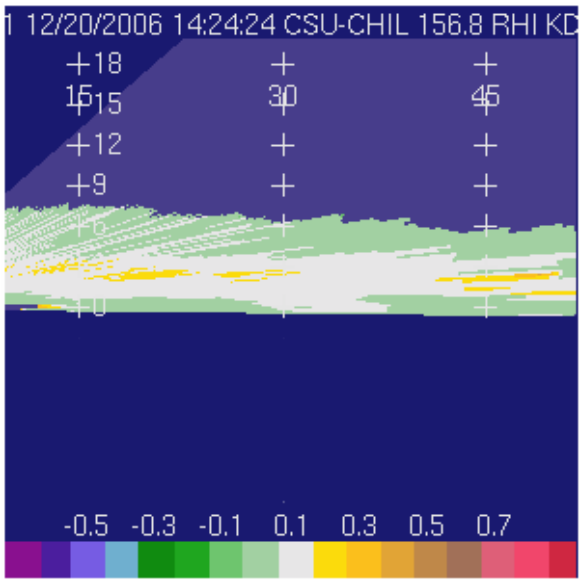

Fig 4b: Kdp (^{o} km^{-1}) RHI at 1424 on 20 Dec 2006

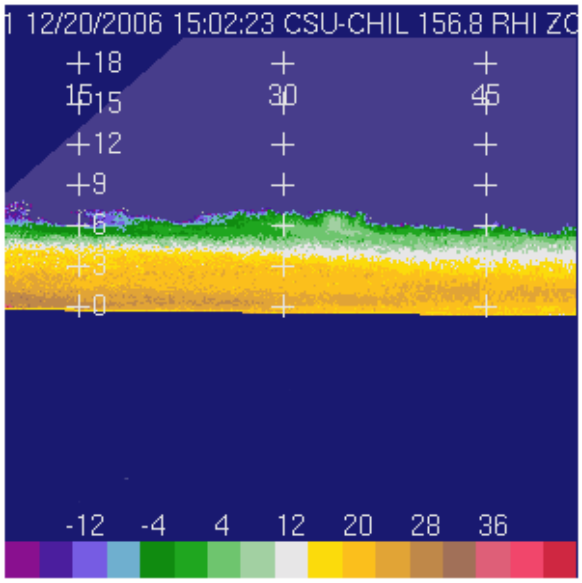

Fig 5a: dBZ RHI 1502 UTC 20 Dec 2006

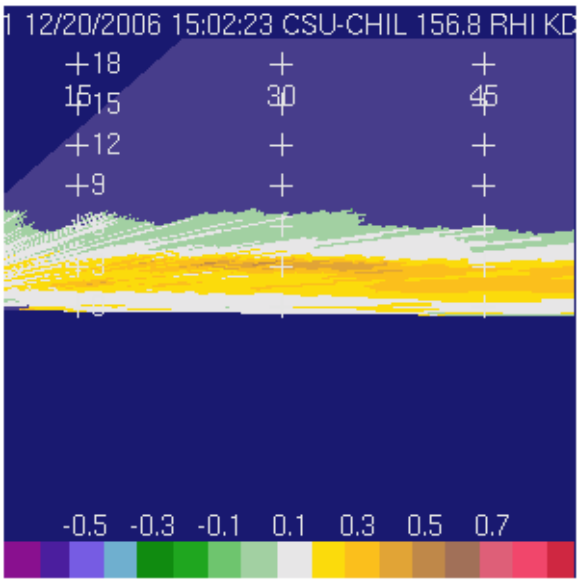

Fig 5b: Kdp (^{o} km^{-1})RHI at 1502 UTC 20 Dec 2006

3. 18 MARCH 2003 STORM OBSERVATIONS

During the period of 16 – 20 March 2003, snow accumulations of historic proportions took place over the western half of the CSU-CHILL radar's standard 150 km operating range (Poulos et al., 2003). One 12 hour period of heavy snow (hourly liquid equivalent precipitation amounts of ~3.2 mm or more measured in Fort Collins) began during the afternoon hours of 18 March 2003. Figure 6a shows the reflectivity field on the 4.23^{o} PPI surface at 1844 UTC. Range rings have been added at the locations where the beam height reaches the -10, -15, and -20^{o}C heights in the 12 UTC 18 March sounding at North Platte NE (LBF). (No Denver sounding was available at this time.) Due to the several hundred km distance between LBF and the radar observation area, the indicated temperature level heights are only approximations. At 1844 UTC, an area of 20 – 30 dBZ reflectivities was approaching the CHILL radar from the southeast (Fig. 6a). The corresponding Kdp field contained an area of >0.2 ^{o}km^{-1} values in the approaching echo mass (Fig. 6b).

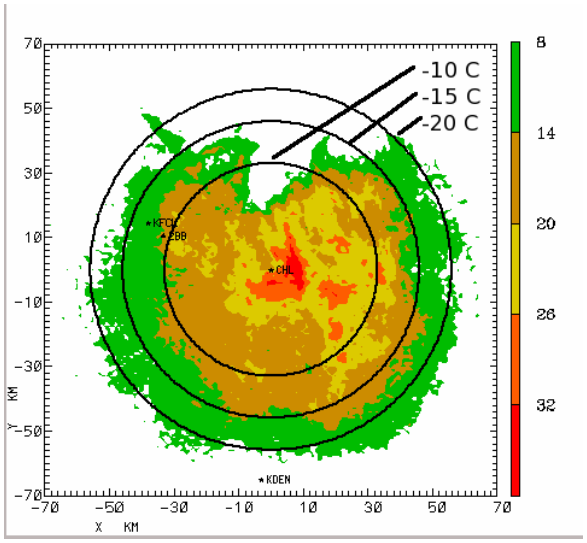

Fig 6a: 4.2^{o} PPI: dBZ at 1844 UTC on 18 Mar 2003

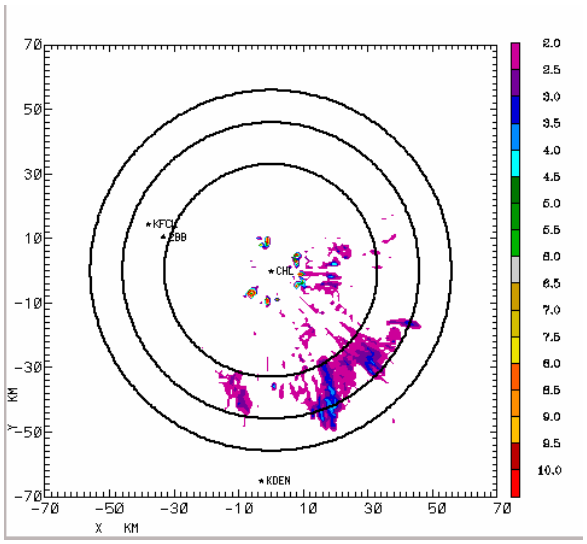

Fig. 6b: As in Fig 6a except data is Kdp x 10.

By 2004 UTC higher reflectivities had overspread the Fort Collins climate station rain gauge site (marked as KFCL in Fig. 7a). The area of enhanced Kdp values, maximizing roughly near the -15^{o}C temperature level, was present just north of KFCL at as higher precipitation rates were beginning to occur at 2004 (Fig. 7b).

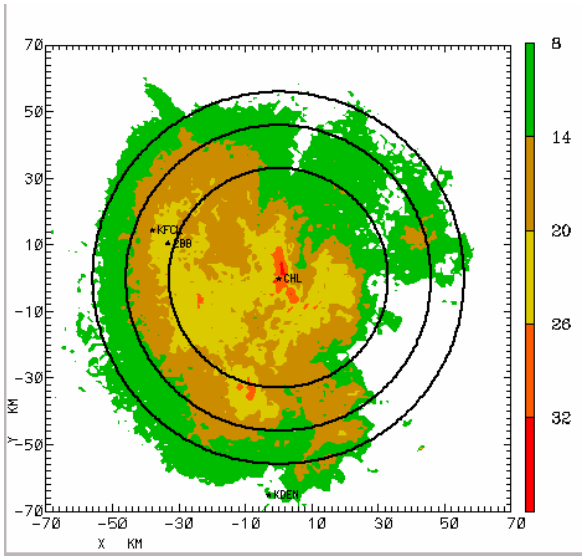

Fig. 7a 4.2° PPI: dBZ at 2004 UTC on 18 Mar 2003

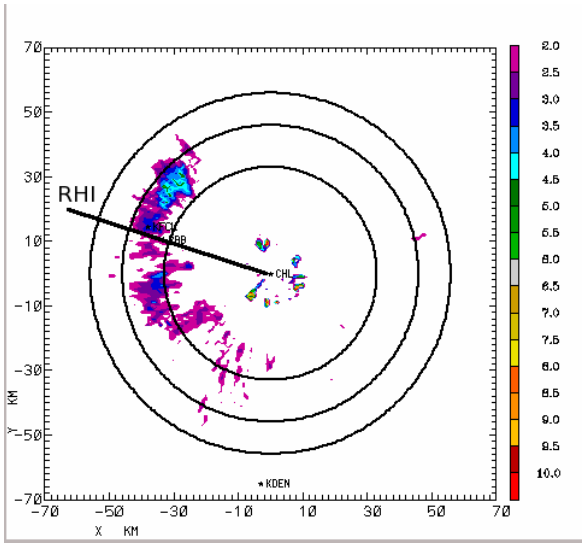

Fig. 7b As in 7a except data is Kdp x 10.

RHI observations made on the general direction of KFCL at 1943 UTC (azimuth 287.6) are shown in the various panels if Figure 8. This scan intercepted the higher reflectivity area that was moving towards Fort Collins. As in the 20 December 2006 shown in section 2, reflectivities generally increase towards the surface. The reflectivity pattern also contains evidence of locally higher values in a precipitation "streamer" visible in the 15 – 25 km range interval.

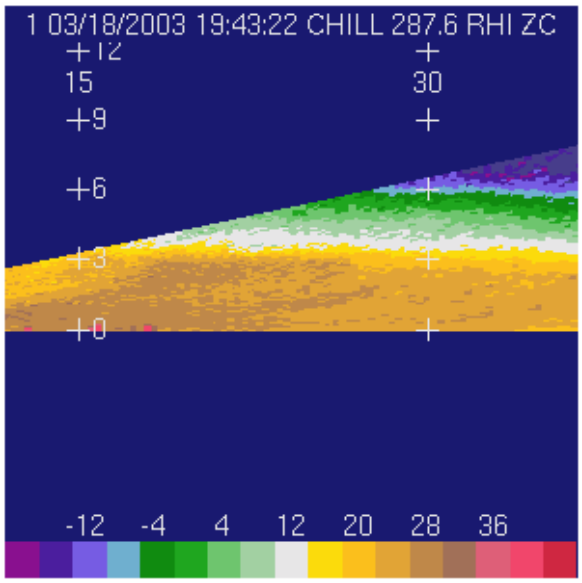

Fig 8a: dBZ at 1943 UTC on 18 Mar 2003

A layer of general Kdp enhancement was present near the 3 km AGL height (Fig. 8b). A localized region of Kdp values reaching 0.4°km^{-1} was present in association with the streamer echo.

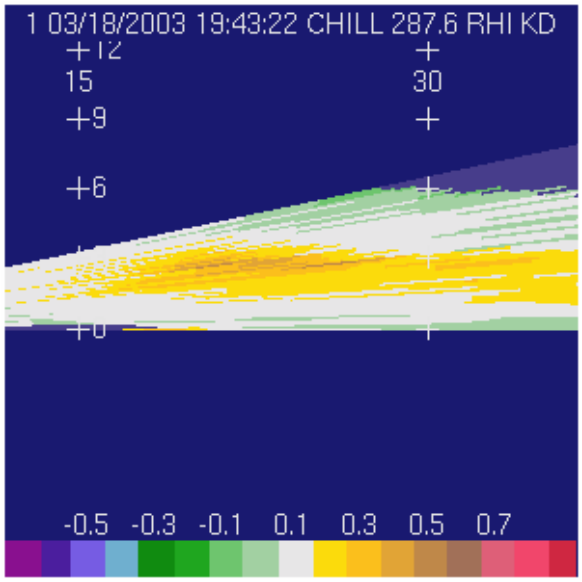

Fig. 8b: Kdp (° km^{-1}) at 1943 UTC on 18 Mar 2003

In concert with the detection of the positive Kdp layer, the differential reflectivity field also showed evidence of oblate particles aloft, with the Zdr values reaching ~1.5 dB in the general vicinity of the maximum positive Kdp layer (Fig. 8c).

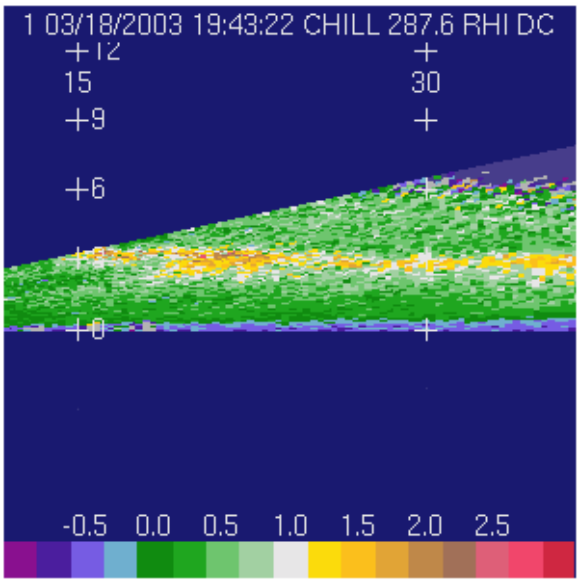

Fig. 8c: Zdr (dB) at 1943 UTC on 18 Mar 2003

Linear depolarization ratio (LDR) measurements of winter season precipitation are often limited by poor signal to noise ratio values in the cross polar reception channel. To remove signal corruption due to noise, a cross polar channel SNR threshold of +10 dB has been applied to the LDR data plotted in Fig. 8d. The largest LDR values (~ -23 to -21 dB) occurred in the upper portion of the precipitation streamer. These LDR levels indicate the existence of relatively high bulk density, non-spherical particles that are undergoing significant fluctuations in their spatial orientations.

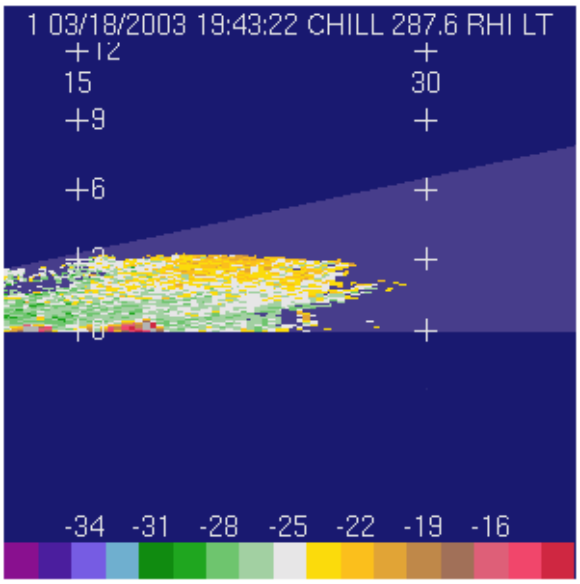

Fig 8d: LDR (dB) at 1943 UTC on 18 Mar 2003

4. HEIGHT PROFILES

A more detailed view of the vertical structure of the various radar fields can be constructed from the RHI scan data. A Cartesian grid point representation of the RHI data was developed by using the NCAR REORDER program. Figure 9a shows the vertical profiles obtained in the 16 – 24 km range interval (i.e., centered on the precipitation streamer) of the RHI scan shown in Fig 8. The maximum Kdp values occur at 4.1 km MSL; the Zdr and LDR peaks are a few hundred meters higher (4.7 km). These dual polarization data maxima occur in the general -12 to -16°C temperature range. (Recall that the temperatures in the March 2003 case are based on the LBF sounding.)

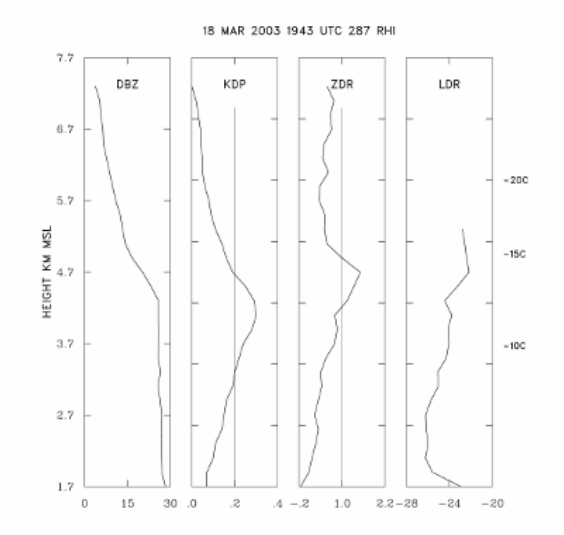

Fig 9a: Vertical radar data profiles at 1943 UTC on 18 Mar 2003. Temperatures along the right edge are from the 12 UTC North Platte sounding.

Similar vertical profiles from the 20 December 2006 case for the 20 – 28 km range interval are plotted in Fig. 9b. The Kdp maximum is again found near the -15°C level, with the most positive Zdr values occurring at a slightly greater altitude. (Weak cross polar signal levels restrict usable LDR observations to the lowest ~1 km.)

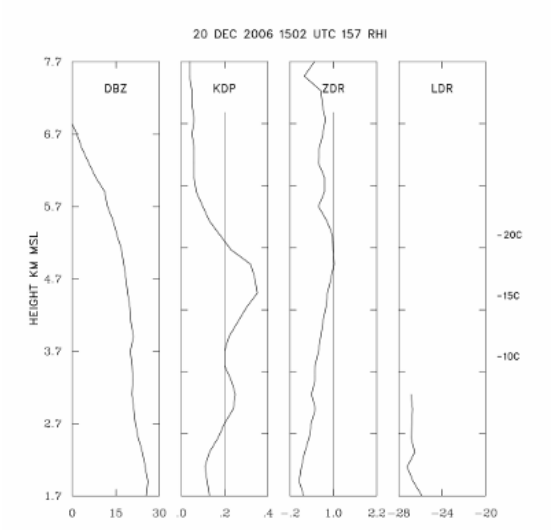

Fig 9b: Radar data profiles at 1502 UTC on 20 Dec 2006. Temperatures along the right edge are from the 12 UTC Denver sounding.

Qualitatively, the maxima in the Zdr and Kdp profiles are likely related to the presence of ice crystals with generally planar shapes whose growth pattern probably included the development of dendritic extensions. The quasi-horizontal fall orientation of these particles produces positive Zdr values. Sufficient concentrations of such particles can generate detectable differential propagation phase shifts and consequently positive Kdp values. At lower heights where particle aggregation is active, the hydrometeor population shifts away from quasi-planar ice crystal shapes towards less distinctive, reduced bulk density aggregates (Lo and Passarelli, 1982). The quasi-spherical shapes and lowered densities of these composite ice / air aggregates causes the Zdr and Kdp values to tend towards zero.

5. BACKSCATTERING MODEL RESULTS

To aid in interpreting the radar data height profiles, a microwave backscattering model was used to calculate the radar observations expected from various populations of ice hydrometeors. This scattering model is based on the T-matrix methods of Waterman (1971).

The first general category of scattering model runs was focused on the Kdp magnitudes that might be generated by dendritic crystals. This crystal habit was selected since it has a growth rate maximum at approximately -15^{o}C under water-saturated conditions (Fukuta and Takahashi, 1999). The fixed, background model parameters were a temperature of -15^{o}C, a radar wavelength of 11 cm and a fixed elevation angle of 3^{o}. The scatterers were also assumed to have a Gaussian distribution of canting angles with a mean value of 0^{o} and a standard deviation of 20^{o}. Ten particle diameters were considered (0.2 to 2.0 mm in increments of .2 mm). Following Lo and Passarelli (1982), an exponential size distribution with a relatively steep slope parameter (λ=30 cm^{-1}) was prescribed to simulate a pre-aggregation situation. Sixteen scattering model runs were then made involving various combinations of particle axis ratios (height / width) and bulk densities typical of dendrites. The results of these simulations are summarized in Figure 10. For the prescribed particle concentrations, Kdp values of ~0.15^{o}km^{-1} are generated when the dendritic particles have axis ratios of ~0.15 or less and when they are able to attain bulk densities greater than 0.2 g cm^{-3}. Dendritic densities on this order have been reported (Heymsfield, 1972). Also, encounters with riming conditions could increase the bulk densities beyond the low values expected for the basic dendrite particle habit. The Kdp values are concentration-dependent, but the range of calculated reflectivity levels (~12 – 20 dBZ) is plausible. These calculations indicate that suitable collections of dendritic particles can produce S-Band Kdp values of a few tenths of a degree per km.

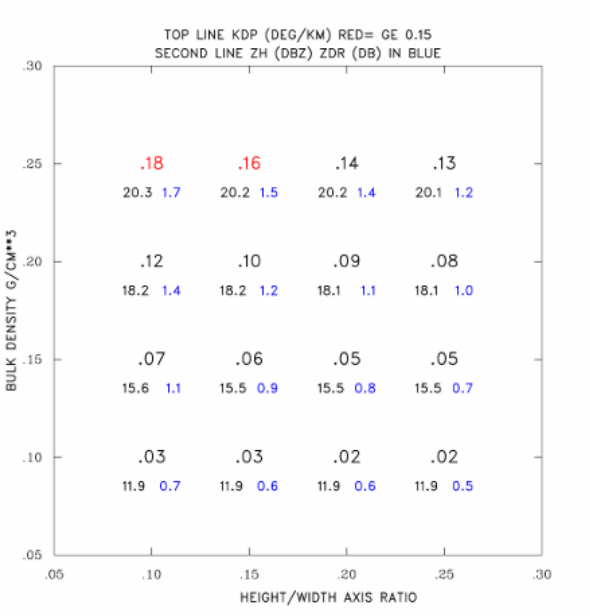

Fig 10: 16 run T-Matrix results for dendritic particles

The second category of scattering model runs attempted to simulate a broader (i.e., not exclusively dendritic) range of particle habits. In these simulations, the particle densities decreased from .9 to .1 g cm^{-3}, and the axis ratio increased from 0.1 to .85 across the 0.2 to 2.0 mm diameter range. This variation was designed to include both small, high density, pristine crystals as well as larger diameter, low density aggregates. To represent the collection effects of the aggregates, the intercept and slope parameters of the exponential particle size distribution were reduced

from the values used in the “dendrites only” model runs. The results are summarized in Table 1:

Table 1: Results of T-matrix model run simulations of snow particle aggregation

Radar measurand	Aggregated snow distribution
Zh (dBZ)	18.7
Zdr (dB)	0.3
Kdp ($^{o}km^{-1}$)	.09
rhoHV	.991
LDR (dB)	-27.8

The radar values calculated from this generic aggregated snow particle population include relatively small Kdp and Zdr magnitudes. This is in general agreement with the dual polarization data values observed by the CSU-CHILL radar in the lower portions of the height profiles shown in Figs 9a and 9b.

6. CONCLUSIONS

The data collected by the CSU-CHILL radar in two major winter storm events contained indications that organized areas of S-Band Kdp values on the order of 0.2^{o} km^{-1} existed in association with echo regions that were known to have produced heavy snowfall rates at the surface. The maximum positive Kdp values were generally found to occur near the $-15^{o}C$ level, a temperature regime where rapid growth of dendritic crystals can be expected in a water saturated environment. The scattering model results indicate that sufficient concentrations of dendritic particles, especially when they are of relatively high bulk density, can generate Kdp values of the observed magnitudes. The detection of these positive Kdp regions near the $-15^{o}C$ temperature level may be useful in the identification of regions of active snow particle growth in winter storm systems.

References:

Fukuta, N. and T. Takahashi, 1999: The growth of atmospheric ice crystals: A summary of findings in vertical supercooled cloud tunnel studies., J. Atmos. Sci., 56, 1963-1975.

Heymsfield, A. J., 1972: Ice crystal terminal velocities., J. Atmos. Sci., 29, 1348-1357.

Miller, L. J., C. G. Mohr, and A. J. Weinheimer, 1986: The simple rectification of Cartesian space folded radial velocities from Doppler radar sampling. J. Atmos. Oceanic Technol., 3, 162-174.

Mohr, C. G. and R. L. Vaughan, 1979: An economical procedure for Cartesian interpolation and display of reflectivity data three-dimensional space. J. Appl. Meteor., 18, 661-670.

Poulos, G. S., D. A. Wesley, M. P. Meyers, E. Szoke, and J. S. Snook, 2003: Exceptional mesoscale features of the Great Western Storm of March 16-20, 2003. American Meteorological Society- 10^{th} Conference on Mesoscale Processes, Portland, Oregon, 23-27 June, paper 14.2A (available in the online permanent archive of the AMS)

Ryzhkov, A. V. and D. S. Zrnic, 1988: Discrimination between snow and rain with a polarimetric radar. J. Appl. Meteor, 37, 1228-1240

Trapp, J. R., D. M. Schultz, A. V. Ryzhkov, and R. L. Holle, 2001: Multiscale structure and evolution of an Oklahoma winter precipitation event. Mon. Wea. Rev., 129, 486-501.

Waterman, P. C., 1965: Matrix formulation of electromagnetic scattering. Proc. IEEE, 53, 805-812.

Wang, Y., and V. Chandrasekar, 2009: Algorithm for estimation of specific differential phase., J. Atmos. and Ocean, Tech., in press

Acknowledgments:
Dr. Brenda Dolan of the CSU Atmospheric Science Department provided valuable assistance in running the T-matrix model.
The CSU-CHILL National Radar facility is supported by NSF ATM 0735110.